SHALE DIAGENESIS IN THE BERGEN HIGH AREA, NORTH SEA

J. Reed Glasmann, Steve Larter, Nowell A. Briedis,
and Paul D. Lundegard

UNOCAL Science and Technology Division, 376 South Valencia Boulevard
Brea, California 92621

Abstract—Illite diagenesis in Tertiary and Mesozoic shales in the Bergen High area, northern North Sea, was studied using mineralogic, isotopic, and computerized thermal modeling techniques. The Tertiary shales are dominated by smectite, with lesser amounts of illite, kaolinite, and chlorite. At present burial temperatures of >70°C smectite is absent, and the shales contain abundant lath-shaped illite which yields a mixed-layer illite/smectite (I/S) X-ray powder diffraction (XRD) pattern. Transmission electron microscopy (TEM) indicates that the illite laths increase in abundance and thickness with increasing depth; XRD patterns indicate a progressive increase in the illite component of the I/S. The deepest samples were found to contain long-range ordered (R=3) I/S, which showed platy particle morphology with the TEM. K-Ar ages of most of the <0.1-μm-size illite separates imply that illitization was a relatively brief event affecting a thick sequence of sediments during late Cretaceous to early Paleocene time (65–87 Ma); however, measured ages were affected by trace levels of detrital Ar contamination and do not represent the true age of diagenesis.

Several methods of quantifying Ar contamination were used to correct measured ages to obtain a reasonable estimate of the true age of diagenesis. The corrected ages are imprecise due to uncertainties in quantifying the levels of sample contamination, but generally suggest a Paleogene (38–66 Ma) period of illitization. In contrast, simple kinetic models of smectite-illitization suggest much younger ages of diagenesis (0–40 Ma at the Veslefrikk field; 0–60 Ma at the Huldra field). The timing of the diagenesis and the morphologic aspects of the authigenic illite suggest that illite precipitated before late Tertiary compaction and resulted in a decrease in fluid permeability. Low trapping efficiency of early Tertiary sediments, vertical escape of warm fluid from the Brent sandstone, and high heat flow may have promoted illite diagenesis in the shales prior to deep late-Tertiary burial.

Key Words—Diagenesis, Illite, Illite/smectite, K-Ar ages, Shale, Transmission electron microscopy.

INTRODUCTION

Tertiary and Mesozoic sediments overlying Brent Group sandstones in the Bergen High area, northern North Sea, consist largely of hemipelagic mudstones and marls, the combined thickness of which locally ranges from 2 to 4 km and exceeds 4–5 km in the adjacent Viking graben (Glasmann *et al.,* 1989a; Thomas *et al.,* 1985; Goff, 1983) (Figure 1). Organic-rich shales of the Humber Group (Kimmeridge-Draupne formations) comprise the major source rocks for hydrocarbons in the northern North Sea and have been widely studied to determine maturation history (Dahl and Speers, 1985; Field, 1985; Thomas *et al.,* 1985; Goff, 1983). Fewer studies are available on the diagenetic changes affecting shale mineral assemblages in the northern North Sea, but reconnaissance work indicates progressive depth-temperature-related changes in the clay mineralogy (Dypvik, 1983; Pearson *et al.,* 1982). A general assumption in these studies has been that the clay mineral assemblages are in equilibrium with the present thermal-chemical environment and that progressive changes in mineralogy (i.e., smectite-to-illite reaction) arise from progressive changes in the burial environment through time; however, in basins such as the North Sea that have complex thermal or fluid-migration history, changes in the clay mineral assemblage may record older diagenetic episodes, not the present environment, as has been shown elsewhere (Elliott and Aronson, 1987; Aronson and Lee, 1986; Morton, 1985; Hoffman *et al.,* 1976).

This paper is part of a study of clay mineral diagenesis in the Bergen High area and focuses on the diagenesis of Tertiary and Mesozoic shales overlying Brent Group sandstones at the Huldra, Veslefrikk, and Oseberg fields in the Norwegian sector of the northern North Sea (Figure 1). The goals of the study were: (1) to characterize the clay mineral assemblages of post-Brent shales and to determine their present relationships to basin temperature and organic maturation; (2) to determine the history of illite diagenesis by means of K-Ar dating of illitic clay separates; (3) to model the process of shale diagenesis and its relation to fluid migration in the Brent sandstone; and (4) to contrast North Sea shale diagenesis with diagenetic trends in shales from other sedimentary basins.

SAMPLES AND ANALYTICAL METHODS

Cuttings and conventional core from eight wells from the Huldra, Veslefrikk, and Oseberg fields were studied. Samples were analyzed by a variety of techniques, including petrographic, transmission electron microscopic, X-ray powder diffraction (XRD), and K-Ar analyses. Standard petrographic thin sections of conventional core samples from five wells
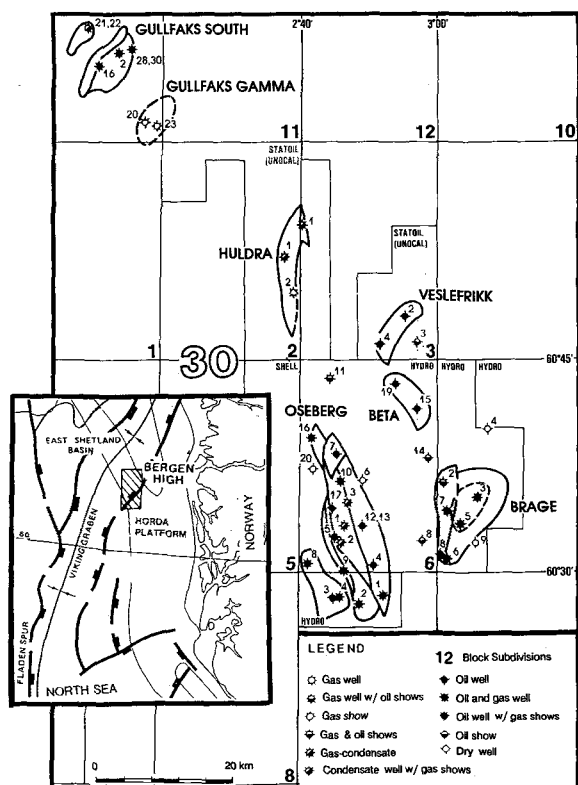
Figure 1. Location of major fields and wells studied in the Bergen High area, North Sea.

were prepared after impregnating the samples with blue-dyed epoxy. Feldspars were stained according to the method of Friedman (1971), and calcite was stained according to the method of Dickson (1965). The samples collected for this study were cleaned of hydrocarbons by a reflux-solvent technique, if appropriate. The modal composition of sandstone samples was determined by point counting at least 300 points per slide.

Clay minerals were separated after disaggregation of the samples by gentle grinding and mild sonic treatment. Hydrocarbons were extracted by treating the disaggregated samples several times with a solvent containing 70% toluene, 15% acetone, and 15% methanol. The samples were washed with this solvent using a blender and centrifuged, and the extract was decanted, repeating this procedure until the extract was clear. Following hydrocarbon extraction, the samples were dried at room temperature and then dispersed in distilled water. The clays were separated by centrifugation using spin times calculated for the settling of spherical particles. The 20–2-, 2–0.5-, 0.5–0.2-, 0.2–0.1-, and <0.1-μm-size fractions were isolated and saturated with Mg by several washes with 0.5 M $MgCl_2$. Excess salt was removed by washing the samples with water and absolute methanol, and slides for XRD analysis were prepared by a smear method (Theisen and Harward, 1962). Slides were analyzed in a constant humidity environment (54% relative humidity) on a Norelco diffractometer (CuKα, 43 kV, 28 mA) using the characterization treatments outlined by Glasmann and Simonson (1985).

Clay mineral abundances were estimated from measured peak heights, and the composition of mixed-layer clays was determined by the method of Reynolds (1980). Illite/smectite structures were modeled using the NEWMOD computer pro-

gram developed by R. C. Reynolds (Department of Earth Sciences, Dartmouth College, Hanover, New Hampshire), and calculated diffractograms of mineral mixtures of illite and I/ S were generated to assess levels of illite contamination of <0.1-μm-size I/S separates. For the samples selected for K-Ar dating, more detailed sample characterization was undertaken using transmission electron microscopy (TEM). Dilute Mg-saturated clay suspensions were pipeted onto glow-discharged carbon/Formvar-coated copper grids, and particle morphology and sample purity were assessed at magnifications ranging from 10,000 to 200,000×. Several specimens were shadowed with gold/palladium using a shadow angle of 20° to measure particle thickness, following the method of Nadeau *et al.* (1984) and McHardy *et al.* (1982). All samples were analyzed on a Hitachi H-600 instrument, operated at 75–100 kV and 15 μA.

Illite K-Ar isotope analyses were made by Paul Damon, University of Arizona, Tucson, Arizona. Potassium analyses were made by atomic absorption on a minimum of three splits of each size-fraction. Argon was analyzed using about 100 mg of clay after pre-baking for 10–12 hr at 250°C. Several duplicate samples were analyzed without pre-baking in another laboratory and showed no significant difference in age compared with the pre-baked samples. Ages were calculated using the abundance and decay constants of Steiger and Jager (1977). All clays were Mg-saturated to minimize interference of exchangeable K (Perry, 1974) and rinsed in absolute methanol until free of chloride.

Geohistory and maturation models were obtained by computer using both constant-thermal-gradient and rift-basin models based on published basin models (Falvey and Middleton, 1981; Sclater and Christie, 1980; McKenzie, 1978). The beta values used to estimate thinning of the continental crust (McKenzie, 1978) were varied from 1.2 to 1.4 in rift models, and present heatflows were varied from 65 to 75 mW/ m^2. Thermal gradients of 35°C/km and 40°C/km were used for the constant gradient models. Organic maturation parameters were calculated using Lopatin-style integration on both decompacted and non-decompacted burial curves, as suggested by Waples (1980). The calculation of vitrinite reflectance was based on the conversion of the time temperature index (TTI) (Royden *et al.*, 1980), modified as suggested by Ritter (1985).

RESULTS AND DISCUSSION

Clay diagenesis in Mesozoic shales

Tertiary shales from Huldra and Veslefrikk have a clay mineral assemblage containing abundant smectite, with lesser amounts of illite, kaolinite, and chlorite (Table 1). Randomly interstratified I/S (R=0, Reynolds, 1980) was found to be a major component of the lower Paleocene-upper Cretaceous shales, and graded into weakly ordered to moderately ordered I/S (R=1) in the mid- to lower Cretaceous section as the proportion of illite layers progressively increased with increasing depth of burial (Figure 2). Pre-Cretaceous shales were characterized by the presence of R=1 I/S, kaolinite, illite, and chlorite. Triassic mudrocks commonly contained a clay mineral assemblage of long-range ordered I/S (R=3 or Kalkberg ordered), and more chlorite, less kaolinite, and no K-feldspar, compared with the shales. In several Triassic samples, kaolinite was absent, and the rock contained only chlorite and illite. Clay assemblages characterized by the presence
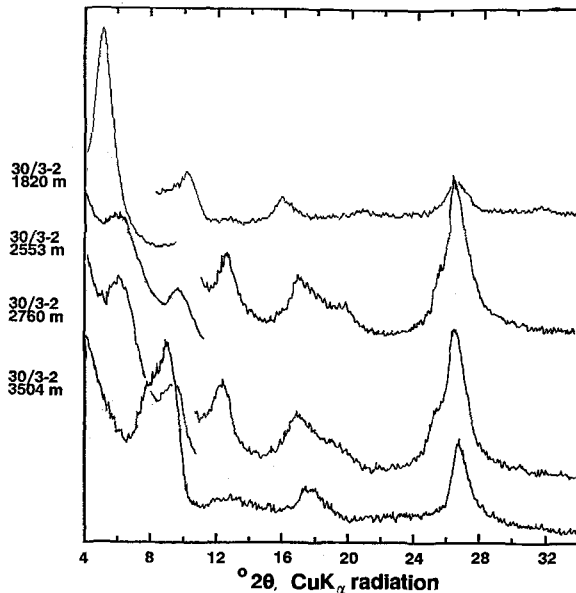
Figure 2. X-ray powder diffraction patterns of representative <0.1-μm-size clay separates from Mesozoic shales, Veslefrikk field, northern North Sea. All patterns represent Mg-saturated, ethylene glycol solvated clays analyzed under constant 54% relative humidity.
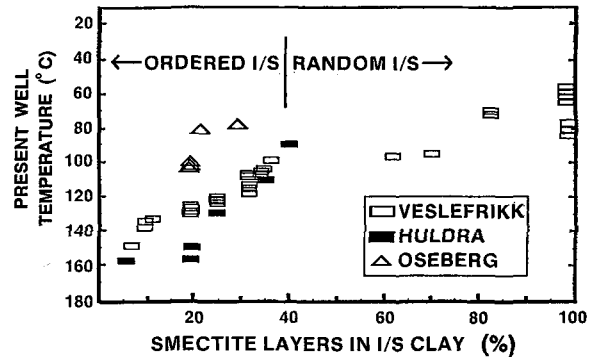

Figure 3. Expandability of illite/smectite (I/S) vs. temperature for shales in the Bergen High area, North Sea. Bottom-hole temperatures were extrapolated from maximum-recorded well log temperature.

of R=3 I/S generally had vitrinite reflectances (VR) of >0.7–0.8% (Table 1).

The relationship between measured well temperature and the percentage of smectite layers in the I/S smectite-rich shales indicates low-temperature burial environments in the Bergen High area (T < 60°–70°C) (Figure 3). Because the clay data were based on the analyses of cuttings, this temperature limit may have been affected by sample contamination due to caving of the well. The difficulty in identifying smectite in mixtures containing highly expandable I/S also hindered the determination of the upper temperature range of smectite stability. Low-temperature, smectite-rich, <0.1-μm-size clay samples consisted largely of minute, extremely thin, lath-shaped crystals (Figure 4), which were contaminated by traces of electron dense iron oxides and platy minerals (e.g., detrital mica and kaolinite, Figure 4A). Variable flocculation of the tiny smectite laths apparently resulted in high density areas in the TEM images (Figure 4A), in which minute laths were resolved at higher magnification (Figure 4B). Estimates of smectite particle thicknesses made from Pt-shadowed samples indicate that many individual smectite laths were about 10 Å thick.

As shown by the data in Figure 5, ordering of the I/S component developed over a present-day temperature range of 80°–110°C, coinciding with a depth interval from about 2300–2560 m at Veslefrikk and Oseberg and 2650–2900 m at Huldra. XRD analyses suggest that the <0.1-μm-size clay fraction consisted almost

entirely of R=1 I/S, with the percentage of expandable layers decreasing from 40 to 20% with increasing depth and temperature (Table 1; Figures 3 and 5). The major morphologic changes of the clay particles within this depth interval were the disappearance of smectite laths and the progressive increase in abundance of lath-shaped illite (Figures 4C, 4D, and 4E). Particle thicknesses for Pt-shadowed samples suggest that typical illite particles ranged in thickness from 20 to 30 Å. Smectite laths were completely absent from the <0.1-μm-size clay fraction at Veslefrikk by a depth of 2760 m, which corresponds to a present-day temperature of about 110°C. A similar temperature relationship was found at Huldra; here, the <0.1-μm-size clay consisted of well-crystallized illite laths, having no apparent smectite component (Figure 4E). Thus, the TEM analyses suggest the presence of (1) a low-temperature clay mineral assemblage of randomly interstratified and weakly ordered I/S, which apparently formed from mixtures of discrete smectite and lath-shaped illite; and (2) a higher temperature assemblage of R=1 I/S, which apparently formed from samples containing only illite laths. These observations of I/S XRD mineralogy and particle morphology are consistent with the hypothesis of interparticle diffraction developed by Nadeau (1985), which suggests that smectite-like behavior may result from the surface properties of minute illite crystals.

The occurrence of long-range ordered I/S in the deepest samples from both the Huldra and Veslefrikk fields coincides with present-day temperatures of 150°–160°C. This temperature range is somewhat cooler than that reported by Hoffman and Hower (1979) and considerably cooler than those reported for R=3 I/S in modern geothermal environments (Inoue *et al.*, 1987). The R=3 I/S-chlorite assemblage is very common in hydrothermal environments at temperatures between 180° and 230°C (Yau *et al.*, 1987a; Jennings and Thompson, 1986). Thus, calculated temperature gradients based on clay mineral geothermometry are different from re-

Glasmann, Larter, Briedis, and Lundegard   *Clays and Clay Minerals*

Table 1. Clay mineralogy of shale samples, Bergen High area, northern North Sea.

Sample depth (m)	Particle size (μm)	Smectite (%)	I/S (%)	Smectite layers (%)	Illite (%)	Kaolin (%)	Chlorite (%)	Vitrinite reflectance (% Ro)	Others
				Huldra field					
30/3-1 Well									
2473	15–2	tr	—	—	25	45	30		Q3, P1, C1
	2–0.5	—	20	40	20	35	25		Q1, P0, C1
	<0.1	—	90	40	<5	tr	<10		
2806	15–2	—	10	<40	30	45	15		Q2, P0, C0
	2–0.5	—	15	35	20	40	25		Q1, P0
	<0.1	—	90	35	<5	tr	<10		
3265	15–2	—	—	—	31	46	23		Q2, P0, C2
	2–0.5	—	5	35	25	35	35		Q3, C2
	<0.1	—	90	25	<5	tr	<10		
3703	15–2	—	10	30	30	30	30		Q2, P1, C0
	2–0.5	—	20	20	20	30	30		Q1, P0, C0
	<0.1	—	95	20	<5	tr	<5	0.9	
30/2-2 Well									
3908	15–2	—	—	—	30	50	20		Q3, P1, D1, PY0
	<0.1	—	90	20	5	tr	5	0.9	
4132.8	15–2	—	—	—	30	50	20		Q2, P0, PY0
	<0.1	—	90	5	?	—	10	0.88	
				Veslefrikk field					
30/3-2 Well									
1520	<2	70	—	100	10	20	tr	0.35	
1670	<2	80	—	100	10	10	tr	0.36	
1740	<2	85	—	100	5	10	tr		
1820	<2	80	—	100	10	10	<5	0.42	
1520–1820	composite sample								
	15–2	30	—	100	25	25	20		
	2–0.5	60	—	100	15	25	<5		
	0.5–0.1	75	—	100	10	15	tr		
	<0.1	99	—	100	—	tr	—		
1880	<2	—	80	80	5	15	<5		
1974	<2	—	65	80	15	15	5		
2019	<2	85	—	100	5	<5	5	0.38	
2070	<2	90	—	100	5	tr	5		
2172	<2	65	—	100	10	15	10		
2265	<2	—	55	70	15	15	15	0.37	
2298	<2	—	45	60	15	15	25		
	casing point								
2361	<2	—	20	38	15	35	30	0.51	
2436	<2	—	10	35	20	40	30		
2508	<2	—	15	35	20	40	25		
2553	<2	—	15	35	15	45	25		
	<0.1	—	90	35	tr	tr	10		
2562	<2	—	15	30	20	35	30	0.48	
2616	<2	—	15	30	20	40	25		
2667	<2	—	15	30	20	40	25	0.54	
2706	<2	—	15	30	20	40	25	0.49	
2715	<2	—	15	30	20	35	30	0.47	
2733	<2	—	15	25	20	40	25		
2751	<2	—	15	25	20	35	30	0.46	
2760	<2	—	15	25	15	60	10		
	<0.1	—	80	35	<5	10	5		
2784	<2	—	15	25	20	35	30	0.44	
2820	<2	—	10	25	20	40	30	0.46	
2862	<2	—	15	20	15	60	10	0.65	
2955	<2	—	15	20	20	55	10	0.67	

Table 1. Continued

Sample depth (m)	Particle size (μm)	Smectite (%)	I/S (%)	Smectite layers (%)	Illite (%)	Kaolin (%)	Chlorite (%)	Vitrinite reflectance (% Ro)	Others
				Veslefrikk field					
30/3-2 Well									
3006	10–2	—	<5	20	25	60	10		
	<2	—	15	20	15	60	10		
	<0.1	—	85	20	<5	10	<5	0.69	
3054	<2	—	15	20	20	40	25	0.67	
3198	<2	—	15	12	25	40	20		
3204	<2	—	15	10	25	35	25	0.72	
3477	<2	—	35	10	50	tr	15		
3504	10–2	—	10	15	75	tr	15		Q0, P0
	<2	—	40	10	40	tr	20		
	<0.1	—	95	8	tr	—	tr		
30/3-4 Well									
2968.6	20–2	—	tr	<40	35	45	20		Q2, K0, P0
	2–0.5	—	10	15	25	50	15		
	<0.1	—	85	20	<5	5	5		
2972	20–2	—	—	—	25	50	25		Q2, K0, P0
	2–0.5	—	10	15	30	45	15		Q0
	<0.1	—	80	17	10	tr	10		
				Oseberg field					
30/6-1 Well									
2355	15–2	—	5	20	15	70	10		Q0, C0
	2–0.5	—	10	30	5	70	15		Vm?
	<0.1	—	70	30	5	25	tr		
2371–2373	15–2	—	tr	—	25	55	20		Q1, P0, K0, Vm?
	2–0.5	—	15	20	20	55	10	0.40	
	<0.1	—	60	20	15	10	15		
30/9-2 Well									
2644	15–2	—	5	30	20	65	10		Q2, K0, P0, S0
	2–0.5	—	20	25	15	55	10		Q0
	0.5–0.2	—	25	20	20	55	tr		
	0.2–0.1	—	50	20	20	30	tr		
	<0.1	—	80	20	5	15	tr		
2676.5	15–2	—	5	25	30	60	5		Q1, K0, P0
	2–0.5	—	15	25	15	70	tr		Q0, K0, P0
	0.5–0.2	—	20	15	20	60	tr		
	0.2–0.1	—	50	18	20	30	tr		
	<0.1	—	85	20	5	10	—		
2770	15–2	—	5	25	25	60	10		Q1, P0, C0, PY
	2–0.5	—	10	20	15	65	10		Q0, P0, PY
	0.5–0.2	—	20	15	15	55	10		
	0.2–0.1	—	55	13	15	25	5		
	0.1–0.05	—	80	15	10	10	—		
	<0.1	—	95	20	<5	<5	—		

Q = quartz, K = K-feldspar, P = plagioclase, C = calcite, D = dolomite, S = siderite, PY = pyrite, Vm = vermiculite. Number following mineral symbol refers to peak intensity: 3 = very intense, 2 = moderately intense, 1 = low intensity, 0 = very low intensity or trace. Clay percentages were determined by summing first order clay mineral peak intensities and dividing individual peak intensities by the sum. Values thus determined were rounded off to the nearest 5%.

ported bottom-hole temperatures in the Bergen High area (Figure 6).

The clay minerals having R=3 I/S XRD character were found chiefly as platy particles of variable electron density, resulting from flocculation and overlapping plates (Figure 4F). The extremely electron dense particles shown in Figure 4F are probably iron oxides. The absence of lath-shaped particles may be due to the facts that: (1) Laths were never present in these deep samples, and the platy particles were related to Triassic detrital mineralogy. This hypothesis is not supported by K-Ar data reported in Table 2, which indicate a late Cretaceous age for the <0.1-μm-size illite of Triassic shales. (2) The platy particles were diagenetic, but with unknown precursor minerals. (3) The platy particles were diagenetic and recrystallized from an earlier lath-
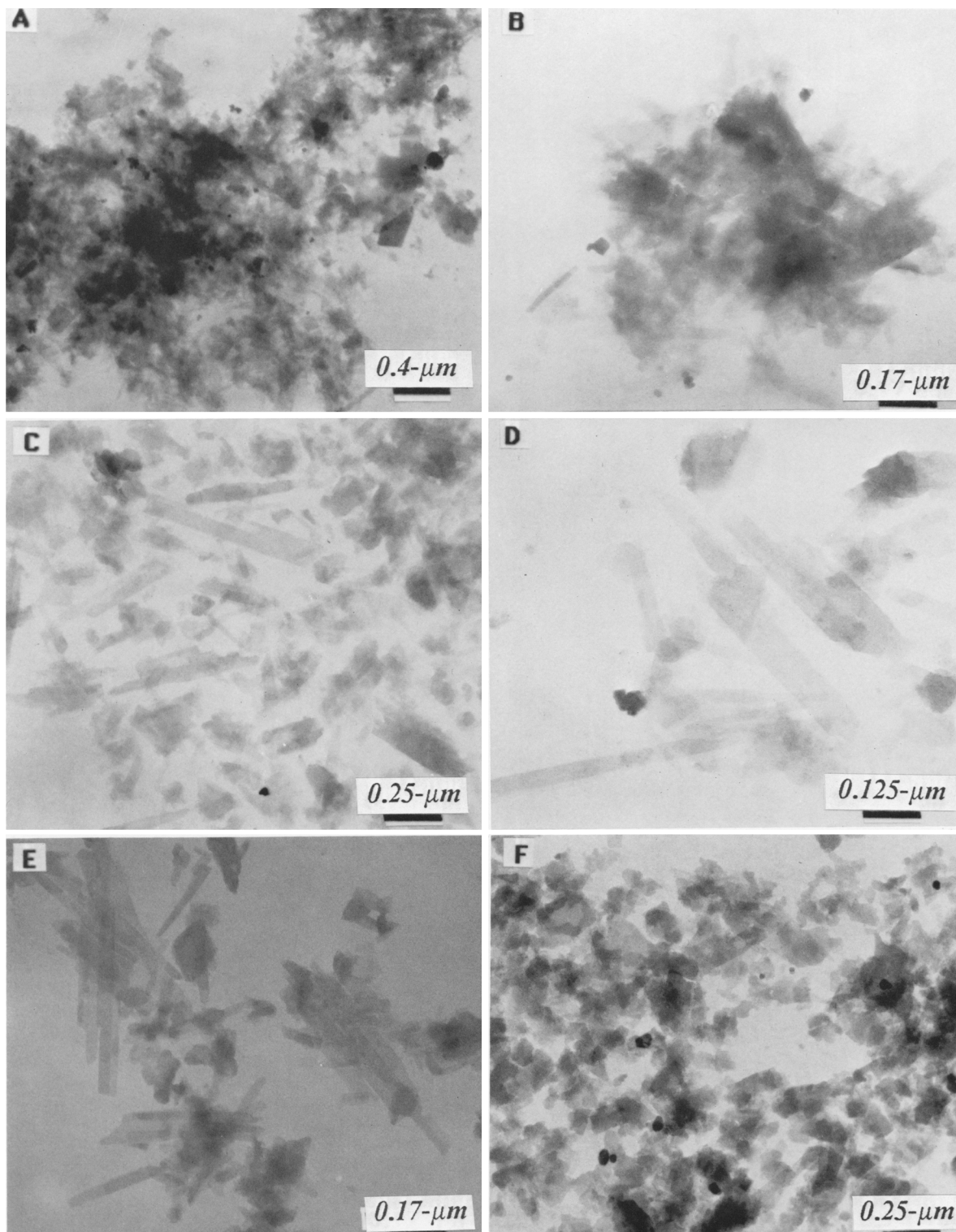
Figure 4. Transmission electron microscope photomicrographs of <0.1-μm-size fractions from shales, Bergen High area, northern North Sea. (A, B) Sample 30/3-2 1520–1820 m, highly smectitic shale. Smectite occurs as extremely thin laths and irregular plates. Larger platy material is probably detrital mica. (C) Sample 30/3-2, 2553 m, illite laths mixed with irregular platy smectite. Illite laths are generally 20–40 Å thick and produce electron images with greater contrast than the thin smectite flakes. (D, E) Abundant, well crystallized illite laths that characterize R=1 illite/smectite (I/S) samples. (D) Sample 30/3-2, 2760 m, lower Cretaceous shale. (E) Sample 30/3-1, 2860 m, very well crystallized laths common in upper Cretaceous shale. (F) Sample 30/3-2, 3504 m, fine clay from Triassic shale at Veslefrikk is characterized by fine platy illite and chlorite.

102
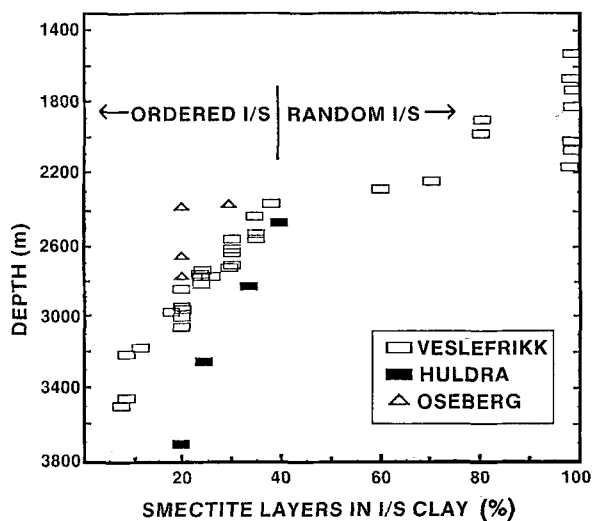
Figure 5. Expandability of illite/smectite (I/S) vs. depth for shales in the Bergen High area, North Sea. Development of ordered I/S occurs at shallower depth at Veslefrikk and Oseberg than at Huldra, reflecting the higher heat flow in the vicinity of these fields.
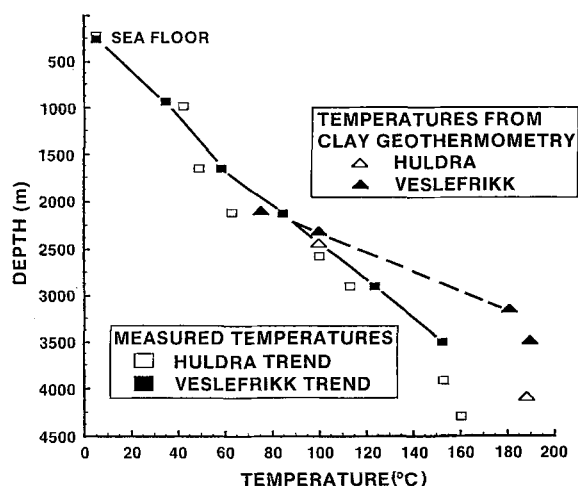

Figure 6. Measured vs. calculated thermal gradients in the Bergen High area, North Sea. Calculated temperature gradients were based on the mineral temperature correlations suggested by Hoffman and Hower (1979).

rich illite assemblage. Studies of hydrothermal mineralization indicate that platy R=3 I/S-chlorite assemblages apparently formed diagenetically by the recrystallization of lower temperature, lath-rich illite assemblages (Inoue *et al.,* 1987; Yau *et al.,* 1987a; Glasmann, 1987b), thereby supporting the idea that the R=3 I/S in the Bergen High area is diagenetic. The diagenetic origin of Bergen High R=3 I/S is also supported by the K-Ar isotopic data (*vide infra*).

Compositional trends in I/S have been used as geothermometers in several sedimentary basins (Dypvik, 1983; Hoffman and Hower, 1979). Temperatures ranging from 80° to 140°C have been correlated with the occurrence of R=1 I/S, suggesting that temperature is not the only factor affecting the illitization of shales (Ramseyer and Boles, 1986); however, given the similar Tertiary burial history of oilfields in the Bergen High area, approximate thermal gradients should be obtainable from clay compositional trends. Calculated thermal gradients in the Bergen High area were constructed using isograds based on temperatures of the disappearance of smectite (70°C), the first occurrence of R=1 I/S (100°C), and the first occurrence of R=3 I/S (180°C, Hoffman and Hower, 1979). A comparison of measured and calculated thermal gradients from the Huldra and the Veslefrikk fields suggests that the calculated gradients provide a reasonable estimate of current well-bore temperatures in the upper part of the section; however, the agreement between measured and calculated gradients is poor for deeper, older shales that contain R=3 I/S (Figure 6). The calculated gradients suggest that the thermal gradients at Veslefrikk were higher than those at Huldra, as evidenced by the shal-

lower depth of the onset of R=1 I/S at Veslefrikk (Figure 5), but nowhere on the Bergen High have burial temperatures been measured that approach the 180°C level suggested by the occurrence of R=3 I/S. Interpretations of clay mineral-temperature correlations usually assume that the clay assemblages are in equilibrium with existing thermal-chemical conditions (Dypvik, 1983; Pearson *et al.,* 1982); however, clay compositional variations can also reflect diagenetic conditions of past burial environments. In sedimentary basins with complex heat-flow history (i.e., rifted basins), diagenetic reactions may be driven by relatively short-lived thermal events reflecting either regional high heat flow or local hydrothermal processes. To interpret clay mineral/temperature relationships properly, the timing of the diagenesis must be established and the nature of the burial environment during diagenesis must be reconstructed (Morton, 1985).

K-Ar age of illitic clays in Mesozoic shales

Potassium-argon dating of illitic minerals in shales has been used to help interpret the timing of illitization and the thermal and diagenetic history of sedimentary basins (Aronson and Lee, 1986; Elliott *et al.,* 1986; Lee, 1984; Aronson and Hower, 1976). Complete isolation of the diagenetic and detrital components in shale clay separates is much more difficult than in sandstones, where diagenetic components are typically much finer-grained than the detrital clasts. Because of size similarities between detrital and diagenetic illitic clays in shales, sample contamination is an ever-present problem, and measured K-Ar ages generally have questionable geologic significance (Hower *et al.,* 1963), unless the K-Ar contribution of the contaminating material is quantified.
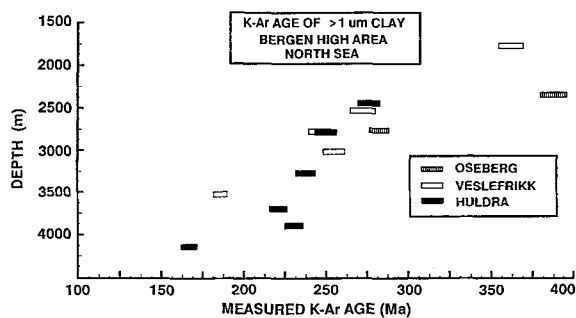
Figure 7.   Plot of illite measured K-Ar age vs. depth for >1-μm-size fractions from Veslefrikk (A) and Huldra (B) fields.

Detrital illite. Detrital illite was found to be most abundant in the coarser size fractions (>2-μm), as evidenced by a relationship of increasing age with increasing particle size (Table 2). In most samples, measured ages were older than depositional ages, but typically much younger than the 400+ Ma muscovites obtained from Brent sandstones in the northern North Sea by Glasmann *et al.* (1989a, 1989b) and Hamilton *et al.* (1987). The oldest measured K-Ar ages were obtained from coarse fractions of highly smectitic shales (361 Ma for sample 30/3-2 at 1820 m and 388 Ma for sample 30/6-1 at 2373 m; Table 2), in which contaminating diagenetic illite was minimal. These ages approach the Caledonian age characteristic of detrital muscovites and overlap ages of slightly chloritized biotite from the Brent (Glasmann *et al.,* 1989a), suggesting that the nondiagenetic fine-silt fraction of the North Sea shales reflects a Caledonian provenance that was slightly altered by pre-depositional weathering. Post-depositional biotite alteration may also give rise to non-stoichiometric loss of Ar (Clauer, 1981); however, post-depositional diffusion of Ar, commonly observed in metamorphic environments (Hunziker *et al.,* 1986), probably did not affect significantly the measured K-Ar ages, given the relatively low burial temperatures encountered in the post-Jurassic sedimentary section in the Bergen High area (Glasmann, 1987a).

The measured ages of illitic silt separates from the Triassic section at Huldra and Veslefrikk were found to be younger than the depositional age (Table 2). Generally, the measured ages of the coarse illite decreased with increasing depth, 276 to 165 Ma at Huldra and 361 to 185 Ma at Veslefrikk (Figure 7). TEM analyses suggest that at least one reason for this age-depth relationship is the increasing amount of undispersed aggregates of diagenetic illite and illitic overgrowths on detrital mica with increasing depth (Figures 8A and 8B). According to Aronson and Hower (1976), the dissolution of detrital feldspar and mica, necessary to provide K for illite diagenesis, will also be reflected in the measured ages of >2-μm-size clay because of the loss of "old" radiogenic Ar and the redistribution of K in

newly formed phases (Aronson and Hower, 1976). At the Huldra field, K-feldspar was absent from shales and sandstones that had been buried >3500 m (unpublished data from this laboratory), and the K-Ar ages of >2-μm-size samples were significantly younger than shallower samples that contained traces of K-feldspar (Table 2). A similar relationship was found for the Triassic section at Veslefrikk field, in which the 185 Ma age of sample 30/3-2 at 3504 m is much younger than the age of overlying shales containing K-feldspar. Thus, the measured K-Ar ages of detrital-rich clay mineral assemblages are probably not representative of the age of the local Caledonian source areas, but were strongly influenced by the presence of younger diagenetic components and loss of old Ar-rich minerals during diagenesis with increasing depth.

Detrital K-bearing minerals also were identified contaminating the <0.1-μm-size fraction of smectite-rich samples and resulted in K-Ar ages that were older than the age of sample deposition (Table 2). The 117 Ma age measured on a 1820-m-deep smectitic shale at Veslefrikk (Table 2) is nearly 60 Ma older than the age of shale deposition (Figure 9), but about 300 Ma younger than the Caledonian age of detrital sources in the northern North Sea. Although detrital mica and feldspar were not evident in XRD patterns of this sample (Table 1), the measured K abundance is consistent with 5–10% contamination by mica or feldspar (Table 2). XRD resolution of low-level mica contamination in <0.1-μm-size clay separates was affected by peak broadening, overlap of I/S diffraction peaks, and possibly interparticle diffraction effects of thin mica flakes. TEM analyses suggested trace levels of contamination by irregular-shaped platy minerals (Figures 4A and 4B), but the absolute amount of such contamination could not be quantified. The 117 Ma age of the smectitic <0.1-μm-size sample suggests that fine-grained micaceous detritus lost considerable radiogenic Ar relative to the illitic detritus in coarser size fractions. Alternatively, the young age may have resulted from the exclusion of detrital feldspar in the <0.1-μm-size fraction or from the uptake of K by degraded micaceous clays. Inasmuch as all clay samples were Mg-saturated prior to K-Ar analysis, exchangeable K in the smectite should not have been a factor in the age calculation.

Diagenetic illite. Measured K-Ar ages of <0.1-μm illitic clays were generally found to be younger than the age of corresponding shale deposition (Figure 9) and ranged from 125 to 64 Ma (Table 2). The measured ages averaged about 67 ± 4 Ma at Veslefrikk and 72 ± 5 Ma at Huldra (Figure 9), defining a geologically brief time interval of I/S ages for such a thick sequence of shales. The measured ages of the <0.1-μm-size clay strongly suggest a diagenetic origin of the lath-shaped and platy illite in shales in the Bergen High area; however, the TEMs suggest the presence of minor to trace

Table 2.   K-Ar ages of illitic clays from Tertiary and Mesozoic shales, Bergen High area, northern North Sea.[1]

Sample	Size (μm)	K (wt. %)	Radiogenic Ar (picomole/g)	Atm. Ar (wt. %)	Age (Ma)	Adjusted age (Ma)	Approximate age of deposition (Ma)
			Huldra field				
2-2 3908	10.0–2.0	2.331	990.0	11.2	230 ± 5		
2-2 3908	<0.1	3.853	515.0	27.1	75.5 ± 1.8	59–65	156
2-2 4132	10.0–2.0	4.647	1396.0	7.9	165 ± 4		
2-2 4132	<0.1	6.128	894.2	7.2	82.3 ± 2	68–75	190
3-1 2473	15.0–2.0	1.612	834.2	6.7	276 ± 6		
3-1 2473	<0.1	2.561	350.2	26.6	77.2 ± 1.8	47–67	78
3-1 2806	15.0–2.0	1.774	826.1	7.9	250 ± 6		
3-1 2806	<0.1	2.992	391.1	25.3	73.9 ± 1.7	49–63	82
3-1 3265	15.0–2.0	1.225	538.5	7.7	237 ± 5		
3-1 3265	<0.1	3.450	474.4	18.5	77.6 ± 1.8	59–67	88
3-1 3703	15.0–2.0	2.161	886.3	7.1	222 ± 5		
3-1 3703	<0.1	3.844	543.6	14.9	79.8 ± 1.9	64–70	150
			Veslefrikk field				
3-2 1820	15–2.0	2.469	1710.8	5.2	361 ± 8		
3-2 1820	2.0–0.5	1.950	978.1	11.4	268 ± 6		
3-2 1820	0.5–0.1	1.896	824.2	16.4	235 ± 5		
3-2 1820	<0.1	1.085	227.3	32.1	117 ± 3		53
3-2 2553	2.0–1.0	1.680	850.8	6.8	271 ± 7		
3-2 2553	<0.1	2.827	321.4	24.0	64.4 ± 1.6	31–53	89
3-2 2760	2.0–1.0	1.843	848.0	14.4	248 ± 6		
3-2 2760	<0.1	2.838	343.6	23.1	68.5 ± 1.6	38–57	150
3-2 3006	10.0–2.0	2.348	1110.0	11.9	254 ± 6		
3-2 3006	<0.1	3.066	384.0	38.8	70.8 ± 1.6	45–60	190
3-2 3504	10.0–2.0	4.652	1573.0	7.3	185 ± 4		
3-2 3504	<0.1	4.970	771.0	18.6	87.3 ± 2.1	73–79	215
3-4 2972	<0.1	4.365	860.9	25.7	110 ± 3	79–106	190
			Oseberg field				
6-1-2373	15.0–2.0	2.634	1977.0	4.9	388 ± 9		
6-1 2371	<0.1	3.689	824.7	10.3	125 ± 3	66–86	188
9-2 2770	20.0–2.0	2.934	1558.0	6.7	282.9 ± 6.5		
9-2 2770	0.2–0.1	3.933	837.4	11.95	118.8 ± 2.7		
9-2 2770	0.1–0.05	4.103	765.9	9.2	104.5 ± 2.4		
9-2 2770	<0.05	4.258	606.6	14.8	80.35 ± 1.83	65–68	190

Atm. Ar = atmospheric Ar.

[1] Adjusted ages represent K-Ar ages corrected for detrital mica and/or K-feldspar contamination.

amounts of detrital mica, indicating that the measured ages were probably affected by the presence of minor amounts of Ar-rich phases. The close grouping of the measured ages at Veslefrikk and Huldra suggests that: (1) the ages were due to the constant level of contamination that overprinted diagenetic Ar contributions so that the diagenetic ages were hidden; and (2) the contamination of detrital Ar was minimal compared with contributions of diagenetic Ar. Hence, the measured ages closely approximate the mean age of illite diagenesis. Possible sources of contamination include Caledonian clay-size mica and recycled lath-shaped illite from eroded Permian sandstones. Erosion of Permian sandstones probably cannot account for the amount of lath-shaped illite present in North Sea shales, but if present in major amounts, such contamination would have resulted in measured ages significantly older than the age of shale deposition. If the sample pretreatments

resulted in similar levels of clay dispersion for all samples, the amount of detrital contamination in the <0.1-μm-size fraction of smectite-rich shales should have been the same as in the illitized samples. The K content of <0.1-μm-size smectite samples should have provided a measure of detrital mica contamination, inasmuch as the smectite contained no fixed K. Such a sample was analyzed from the Veslefrikk field (sample 30/3-2 at 1820 m); the measured K content suggests about 5–10% detrital mica (Table 2), although mica was not evident in XRD patterns of this sample (Table 1). Samples containing poorly ordered I/S contained significantly more K and radiogenic Ar than the smectite-rich clays and gave considerably younger K-Ar ages, due to the addition of K and accumulation of Ar during the duration of the illitization (Table 2). Subtracting the K and radiogenic Ar percentages of the unaltered smectite-rich clays from those of illitized samples yields
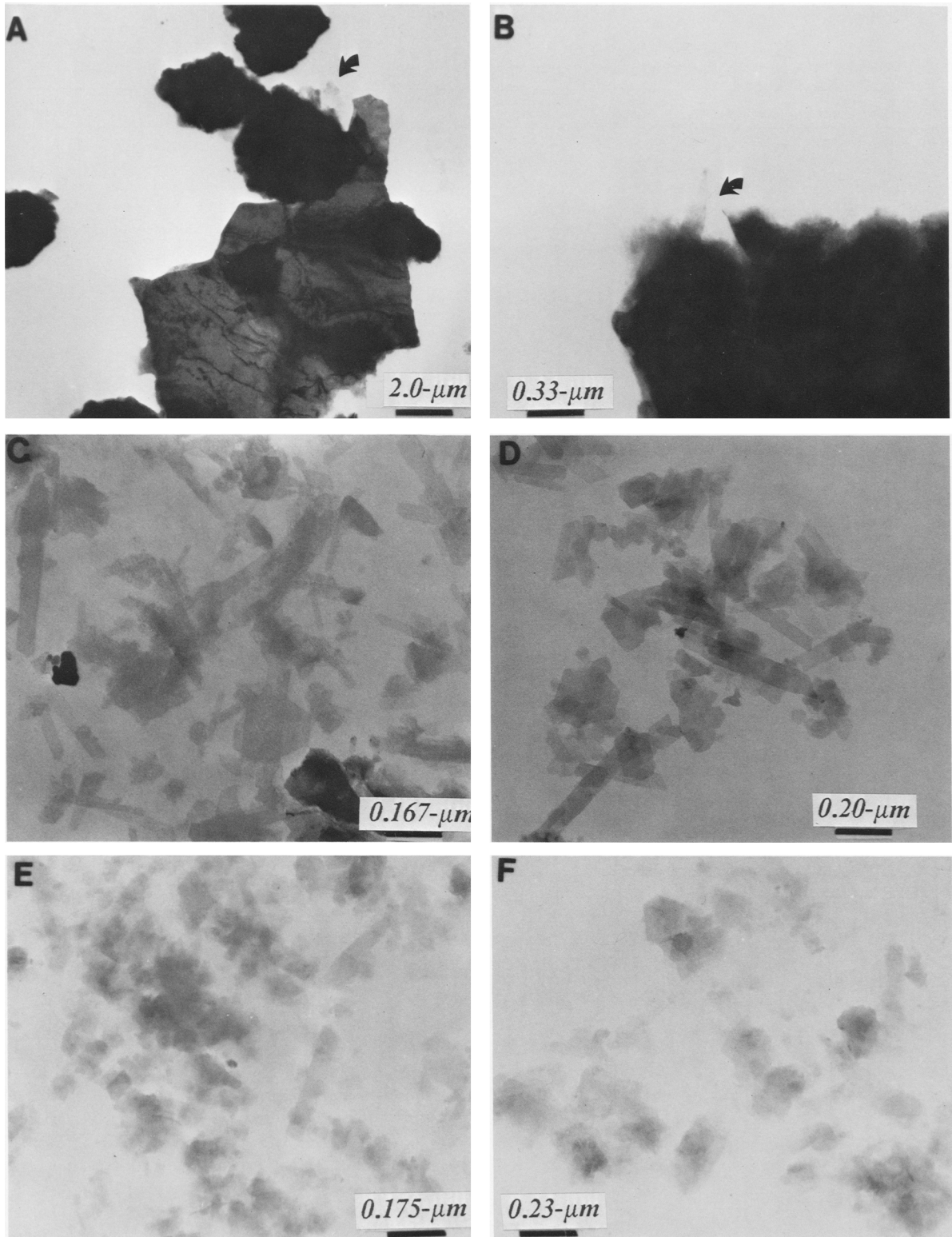
Figure 8. Transmission electron microscope photomicrographs of shale components from various geologic settings. (A, B) Silt-sized separations of shales in the Bergen High area contain detrital platy minerals and undispersed aggregates of finer, probably diagenetic, particles. Diagenetic illite laths also overgrow, or are attached on surfaces of detrital particles (arrow). (C) Lath-shaped diagenetic illite in the <0.1-μm fraction of a hydrothermally altered Pleistocene shale from Imperial Valley, California, sample IV-1, 686 m. (D) Platy illite and chlorite characterize deeper hydrothermally altered samples from Imperial Valley, California, sample IV-1, 1143 m. (E, F) Anhedral platy illite particles from the <0.1-μm-size fraction of deeply buried Pliocene shale, Gulf of Mexico, samples GM-1, 5797 m (E) and GM-1, 6400 m (F).

an estimate of the mean age of the diagenetic components in the sample ("Adjusted age" heading in Table 2). Such a correction assumes that detrital phases were present in constant amount and stable over the range of burial environments represented in this study. Dissolution of fine-grained detrital feldspar and mica, apparent in deeply buried samples in the study area (Glasmann *et al.*, 1989a), should have resulted in a loss of old radiogenic Ar, leading to an underestimation of the mean age of illite diagenesis. Therefore, adjusted ages of <0.1-μm-size I/S probably represent minimum ages of illite diagenesis (Table 2).

Measured K-Ar ages were also corrected by using a mean age of the detrital contamination and an estimate of its abundance. Because Caledonian detritus has apparently lost radiogenic Ar from the <0.1-μm-size fraction as discussed above, ages of 200 and 400 Ma were used to cover a range of possibilities. Because the XRD patterns of <0.1-μm-size clay rarely showed conclusive evidence of mica or feldspar, low levels of contamination were assumed (Table 2). On the assumption that the detrital and diagenetic illite have similar particle densities, a simple mixing equation was used to estimate the effects of detrital contamination. The measured age was therefore the sum of a diagenetic component (age × relative amount) plus a detrital component. Adjusted ages calculated by both of the methods described above are listed in Table 2. The considerable range of adjusted ages for a given sample is due to the many uncertainties involved in assumptions of detrital contamination; however, these adjusted ages are probably minimum ages of diagenesis, because of the apparent high purity of <0.1-μm-size clay suggested by the TEMs and the probable destruction of extremely fine grained detrital sources of K and Ar with increasing depth. The measured K-Ar ages of the <0.1-μm-size illites represent maximum ages of diagenesis, with the most probable age of illitization being between the measured and the adjusted ages.

The measured and adjusted ages of the diagenetic illite in shales in the Bergen High area are inconsistent with illitization in the present temperature-chemical environment. If illite diagenesis was ongoing and in equilibrium with the present thermal environment, adjusted ages should have approached zero in shallow, weakly ordered samples and increased progressively with increasing depth to the point where high temperature recrystallization of R= 1 I/S (illite laths) to R=3 I/S (platy illite) occurred. If the R=1 I/S-to-R=3 I/S transition represents a major structural reorganization, as suggested by the different illite particle morphologies, the Ar clock should have been reset and measured ages should have decreased abruptly. Such an age decrease was not apparent from measured K-Ar ages of the diagenetic illite, suggesting that the R=3 I/S component was not formed at present bottom-hole temperatures. Moreover, the preservation of older ages in
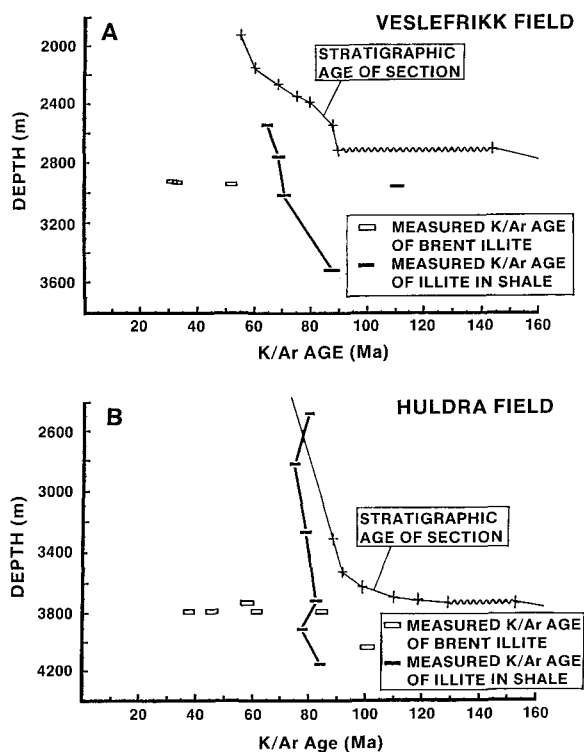

Figure 9. Plot of illite measured K-Ar age vs. depth for <0.1-μm-size clay samples from Veslefrikk (A) and Huldra (B) fields. Saw-toothed line in curves defining stratigraphic age of section indicates a period of erosional unconformity.

the <0.1-μm-size illite at the highest burial temperatures argues against Ar-clock resetting by diffusive Ar loss, even at burial temperatures as high as 150°–160°C.

Modeled illite age. The thermal history of any given strata in a sedimentary basin can be modeled, providing the heat flow, thermal conductivity, porosity, and burial history of the basin are known or can be estimated (Sclater and Christie, 1980; McKenzie, 1978). Assuming that thermal history exerts the primary control on the illitization reactions, the modern I/S composition-temperature relationships (Figure 3) can be modeled through time to predict the mean age of diagenetic illite at a given depth (Figure 10). In the present study, calculated temperature history curves were divided into 10°C increments of illitization based on the present-day I/S-temperature relationships, and the amount of illite precipitated and its corresponding mean age were calculated as shown in Figure 10. As illite diagenesis progressed, new illite precipitated at successively higher temperatures had younger mean ages of precipitation. The mean age of the population of illite precipitated during diagenesis will be the weighted average of the various sub-populations. Thus, the late Cretaceous illitization of smectite that produced a R=0 I/S having 20% I layers accounts for 25% of the total

TEMPERATURE HISTORY PROFILE -TOP CENOMANIAN
30/3-1
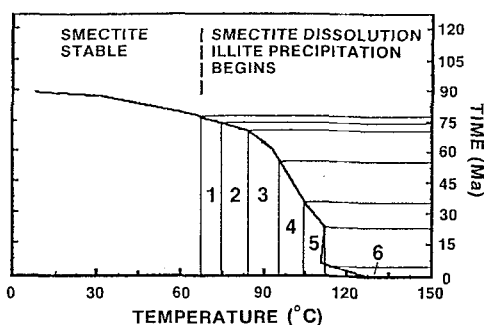
ZONE	TEMPERATURE INTERVAL (°C)	MEAN AGE OF ILLITE IN GIVEN INTERVAL (Ma)	% OF TOTAL ILLITE PPT.	PARTIAL AGE (Ma)
1	65-75	76	25	19
2	75-85	71	15	10.6
3	85-95	63	15	9.5
4	95-105	45	25	11.3
5	105-115	28	10	1
6	115-125	4	10	0.5

MODELED AGE ≅ 52 Ma = SUM OF PARTIAL AGES

Figure 10. Temperature history plot for Huldra field, well 30/3-1, used to calculate the modeled age of illite in Cenomanian shales. The temperature curve is divided into zones representing progressive illitization; weighted mean age of each zone (partial age) is used to calculate modeled age.

illite formed in a Cenomanian shale and had a greater effect on the total radiogenic Ar content of the sample than a similar amount of illite formed during Eocene time (Figure 10). Calculating temperature history curves for a variety of constant and variable thermal-gradient models resulted in a range of "equilibrium" illite ages for a given stratigraphic layer. These "equilibrium" illite ages are compared with measured and adjusted illite ages in Figure 11 and consistently predict younger ages of illite diagenesis than observed. Because the thermal illitization model was based on empirical temperature-I/S relationships that are consistent with current models of illite diagenesis (Bethke *et al.*, 1986; Bethke and Altaner, 1986; Środoń *et al.*, 1986; Velde *et al.*, 1986; Nadeau and Bain, 1986; Morton, 1985), the discrepancy between predicted and measured illite ages strongly suggests that the illitization resulted from thermal-chemical conditions that were not included in the model. Other factors are important during illite diagenesis, including mineral solubility, pore-fluid chemistry, hydrothermal fluid flow, rate of burial, and residence time at a given temperature (Ramseyer and Boles, 1986; Eberl, 1978; Eberl and Hower, 1976) and may have promoted an earlier period of illitization than predicted by the model used in this study.

Thus, the measured K-Ar ages of the <0.1-µm-size illitic clay minerals suggest a diagenetic origin much earlier than that predicted by age modeling based on

current I/S-burial temperatures. Contamination of the fine clay fraction by traces of detrital mica inhibited the accuracy of diagenetic illite-age measurement, but the minimum mean age of diagenesis can be crudely estimated by correcting measured ages for the effects of contamination. The relationship between sample depth and measured age of diagenetic illite indicates that diagenesis of Mesozoic shales was not a result of slow, progressive burial and associated increasing temperature; instead, a relatively constrained period of diagenesis appears to have affected a thick sequence of shales during early to mid Tertiary time.

Relationships to diagenesis in Brent Group sandstones

The illitization time interval defined by the adjusted illite ages overlaps with the time of illite diagenesis and migration of hydrocarbons into the underlying Brent Group sandstone (Figure 11; Glasmann *et al.*, 1989a). Late-stage diagenesis of the Brent included the dissolution of K-feldspar, the precipitation of quartz overgrowth, the growth of diagenetic illite, and the illitization of diagenetic kaolinite (Glasmann *et al.*, 1989a, 1989b; Jourdan *et al.*, 1987; Blanche and Whitaker, 1978; Hancock and Taylor, 1978). Fluid inclusion evidence suggests that quartz cementation was locally facilitated by the migration of warm, saline, compaction water from deeper parts of the Viking graben (Glasmann *et al.*, 1989a; Thomas, 1986; Haszeldine *et al.*, 1984). Wholesale dissolution of K-feldspar and the illitization of kaolinite characterizes the diagenesis of the Brent Group sandstone at depths >3500 m (Glasmann *et al.*, 1989a). The oxygen isotope composition of diagenetic illite in the Brent Group sandstone in the Bergen High area also suggests that illite precipitation was associated with the migration of basin compaction water (Glasmann *et al.*, 1989a), as has been suggested by other North Sea diagenesis studies (Glasmann *et al.*, 1989b; Jourdan *et al.*, 1987). K-Ar ages of diagenetic illite in the Brent suggest a prolonged period of illite precipitation, beginning in the late Cretaceous and continuing into late Neogene time (80 to 27 Ma; Glasmann *et al.*, 1989a, 1989b; Liewig *et al.*, 1987; Jourdan *et al.*, 1987; Thomas, 1986).

Organic geochemistry studies have indicated that hydrocarbon migration from the deep Viking graben may have begun as early as late Cretaceous time (Glasmann *et al.*, 1989a; Dahl and Speers, 1985; Field, 1985; Goff, 1983). Hydrocarbon volumetric calculations suggest a very low trapping efficiency in many Brent reservoirs (Dahl and Speers, 1985), which may have been responsible for the leakage of considerable fluid from Brent reservoirs prior to late Tertiary deep burial and an improvement of sealing mechanisms by compaction. Thermal gradients in the Bergen High area during this period of active hydrocarbon migration have been estimated at between 80° and 100°C/km on the basis

of fluid inclusion data (Glasmann *et al.,* 1989a; Goff, 1983). Thus, leakage of basin compaction fluid (potentially K-rich and warmer than ambient pore fluid) and hydrocarbons at structural highs (e.g., the Huldra, Veslefrikk, and Oseberg fields) could have altered the pore-water chemistry and the thermal environment of poorly compacted overlying mudrocks, thereby promoting the dissolution of smectite and the precipitation of illite during late Cretaceous to early Tertiary time. The escape of migrating basin-compaction water from the Brent may have been limited in time by the accumulation of hydrocarbons and the progressive improvement of the seal overlying the reservoir with continuing Tertiary burial, thereby providing a mechanism for the early shutdown of illite diagenesis in the shales. Such a mechanism may explain the absence of very young illite ages in the <0.1-μm-size clay fraction and the tendency for measured ages of illite diagenesis to define a rather short-lived early Tertiary diagenetic event.

If illite diagenesis was promoted by the thermal and chemical environment produced by the migration of warm compaction water out of the Viking graben, clay diagenesis would not have seriously affected the patterns of organic maturation. The kinetics of vitrinite alteration are much different from those affecting inorganic components. Whereas vitrinite reflectance (VR) measurements are relatively insensitive to short-term perturbations in pore-fluid chemistry or thermal gradient (Middeleton and Falvey, 1983), clay crystal growth can proceed rapidly, given appropriate conditions for precipitation. Because mineral stability is a function of pore-water chemistry as well as temperature, high temperatures are not necessarily required for illitization, if sufficient reactants are supplied; however, the evidence presented in the present study suggests that sufficient thermal and chemical energy for shale illitization could have been supplied by fluid escape from the Brent sandstone during hydrocarbon migration. Subsequent late Tertiary burial has not overprinted the mineralogic record of shale and sandstone diagenesis, but it has influenced organic maturation profiles and the present distribution of hydrocarbons in the Bergen High area (Steven Larter, unpublished data, Unocal Science and Technology, Brea, California). Thus, thermal history reconstructions using VR-based models will not reflect short-lived thermal events, especially if subsequent burial has resulted in present-day thermal conditions similar to those encountered in the past (Goff, 1983).

The morphology of diagenetic illite is also indicative of the general environment of diagenesis. Euhedral, lath-shaped illite is particularly common in sandstones in which crystal growth is unconstrained by pore size. Lath-shaped illite is also abundant in shallowly buried shales that have been hydrothermally altered; it appears to transform to platy illite and eventually to $2M_1$
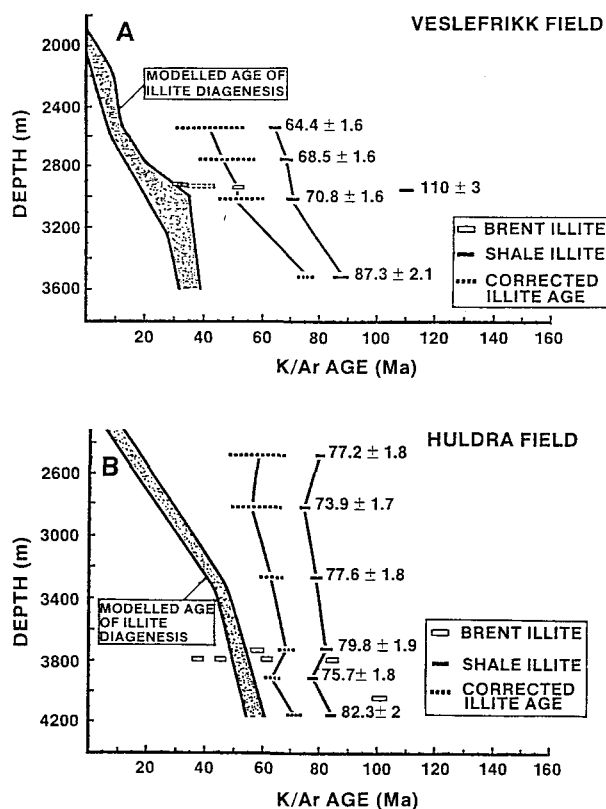

Figure 11. Comparison of measured, adjusted, and modeled illite K-Ar ages at Veslefrikk (A) and Huldra (B) fields, Bergen High area, North Sea.

mica with increasing alteration temperature (Figures 8C and 8D; Glasmann, 1987b; Inoue *et al.,* 1987; Yau *et al.,* 1987b). If present in hydrothermally altered shales, lath-shaped illite suggests alteration temperatures of 130°–180°C, which commonly are found at depths of <1 km. Thus, in hydrothermally altered shales, fluid convection, appropriate fluid chemistry, and lack of compaction promote rapid growth of lath-shaped illite into available pore space.

The morphology of illite from mud-dominated basins having a significant history of compaction is typically anhedral (e.g., Gulf of Mexico; Figures 8E and 8F), even though XRD analyses suggest similar I/S compositions (Figure 12). Anhedral crystals indicate that the illite growth was confined to micropores between adjacent detrital particles or that the illite grew replacively as a host mineral dissolved (Ahn and Peacor, 1986). The predominance of euhedral illite laths in illitized shales in the Bergen High area suggests that diagenesis occurred during the early burial history of the basin, prior to major loss of porosity, in sharp contrast to Gulf Coast-style illitization in which crystal growth was apparently restricted to micropores.
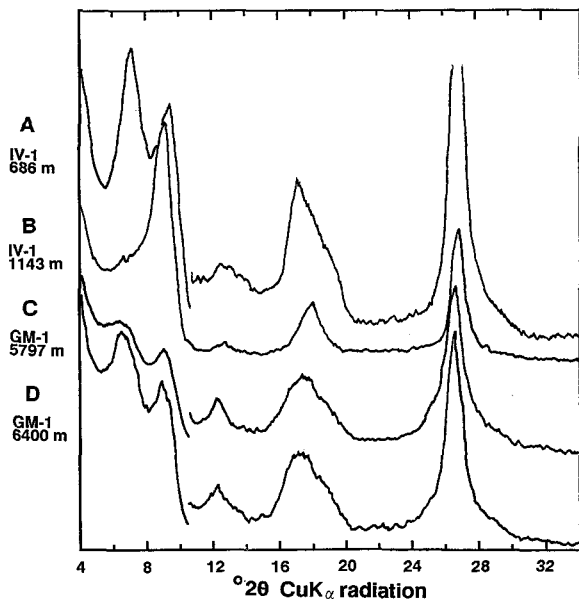
Figure 12. X-ray powder diffraction patterns of <0.1-μm-size fraction from shallow hydrothermally altered Pleistocene shales, Imperial Valley, southern California (A, B) and deeply buried Pliocene shales, Gulf of Mexico (C, D). All patterns represent Mg-saturated, ethylene glycol-solvated analyses obtained under controlled relative humidity (54%). (Cf. Figure 8.)

SUMMARY AND CONCLUSIONS

Illite diagenesis in Mesozoic shales in the Bergen High area is related in time to illite diagenesis in the Brent sandstone reservoir. Euhedral illite growth in shales indicates relatively high shale porosity during diagenesis. Although interpretation of the significance of measured K-Ar ages of <0.1-μm-size illitic clay fraction is complicated by minor amounts of detrital contamination, age-depth trends suggested by adjusted illite ages are useful for contrasting different models of diagenesis. Both measured and adjusted ages of illite diagenesis are earlier than anticipated based on present-day illite-temperature relationships and suggest that the shale diagenesis on structural highs surrounding the Viking graben was influenced by compaction-derived pore fluids during the initial stages of hydrocarbon migration out of the Viking graben. Proper interpretation of clay mineral-temperature relationships requires an understanding of the timing of clay diagenesis and its relationship to basin geologic and fluid-flow history.

ACKNOWLEDGMENTS

REFERENCES

Ahn, J. A. and Peacor, D. R. (1986) Transmission and analytical electron microscopy of the smectite-to-illite transition: *Clays & Clay Minerals* **34,** 165–179.

Aronson, J. L. and Lee, M. (1986) K/Ar systematics of bentonite and shale in a contact metamorphic zone, Cerrillos, New Mexico: *Clays & Clay Minerals* **34,** 483–487.

Aronson, J. L. and Hower, J. (1976) Mechanism of burial metamorphism of argillaceous sediment: 2. Radiogenic argon evidence: *Geol. Soc. Amer. Bull.* **68,** 673–683.

Bethke, C. M. and Altaner, S. P. (1986) Layer-by-layer mechanism of smectite illitization and application to a new rate law: *Clays & Clay Minerals* **34,** 136–145.

Bethke, C. M., Vergo, N., and Altaner, S. P. (1986) Pathways of smectite illitization: *Clays & Clay Minerals* **34,** 125–135.

Blanche, J. B. and Whitaker, J. H. McD. (1978) Diagenesis of part of the Brent Sand Formation (Middle Jurassic) of the northern North Sea basin: *J. Geol. Soc. London* **135,** 73–82.

Clauer, N. (1981) Strontium and argon isotopes in naturally weathered biotites, muscovites, and feldspars: *Chem. Geol.* **31,** 325–334.

Dahl, B. and Speers, G. C. (1985) Organic geochemistry of the Oseberg Field (I): in *Petroleum Geochemistry in Exploration of the Norwegian Shelf,* A. G. Dore, S. S. Eggen, P. C. Home, R. Marne, and B. M. Thomas, eds., Norwegian Petroleum Society, Graham & Trotman Ltd., London, 185–195.

Dickson, J. A. D. (1965) A modified staining technique for carbonates in thin section: *Nature* **219,** 587.

Dypvik, H. (1983) Clay mineral transformations in Tertiary and Mesozoic sediments from North Sea: *Amer. Assoc. Petrol. Geol. Bull.* **67,** 160–165.

Eberl, D. (1978) Reaction series for dioctahedral smectites: *Clays & Clay Minerals* **26,** 327–340.

Eberl, D. and Hower, J. (1976) Kinetics of illite formation: *Geol. Soc. Amer. Bull.* **87,** 1326–1330.

Elliott, W. C. and Aronson, J. L. (1987) Alleghanian episode of K-bentonite illitization in the southern Appalachian basin: *Geology* **15,** 735–739.

Elliott, W. C., Aronson, J. L., and Gautier, D. L. (1986) Bentonite illitization and thermal history, Denver basin, U.S.A.: *Terra Cognita* **6,** 108.

Falvey, D. A. and Middleton, M. F. (1981) Passive continental margins: Evidence for a pre-breakup deep crustal metamorphic subsidence mechanism: *Oceanologica Acta* **4,** 103–114.

Field, J. D. (1985) Organic geochemistry in exploration of the northern North Sea: in *Petroleum Geochemistry in Exploration of the Norwegian Shelf,* A. G. Dore, S. S. Eggen, P. C. Home, R. Marne, and B. M. Thomas, eds., Norwegian Petroleum Society, Graham & Trotman Ltd., London, 39–57.

Friedman, G. M. (1971) Staining: in *Procedures in Sedimentary Petrology,* R. E. Carver, ed., Wiley, New York, 511–531.

Glasmann, J. R. (1987a) Comments on "The evolution of illite to muscovite: mineralogical and isotopic data from the Glarus Alps, Switzerland": *Contrib. Mineral. Petrol.* **96,** 72–74.

Glasmann, J. R. (1987b) Argon diffusion in illite during diagenesis: How good is the K/Ar clock? in *Prog. Abstracts, 24th Annual Meeting, The Clay Minerals Society, Socorro, New Mexico,* p. 60.

Glasmann, J. R., Clark, R. A., Larter, S., Briedis, N. A., and Lundegard, P. D. (1989a) Diagenesis in the Bergen High area, North Sea: Relationships to hydrocarbon maturation and fluid flow, Brent Sandstone. *Amer. Assoc. Petrol. Geol.* (in press).

Glasmann, J. R., Lundegard, P. D., Clark, R. A., Penny, B. K., and Collins, I. D. (1989b) Geochemical evidence for the history of diagenesis and fluid migration: Brent Sandstone, Heather Field, North Sea: *Clay Miner.* **24**, (in press).

Glasmann, J. R. and Simonson, G. H. (1985) Alteration of basalt in soils of western Oregon: *Soil Sci. Soc. Amer. J.* **49**, 262–272.

Goff, J. C. (1983) Hydrocarbon generation and migration from Jurassic source rocks in the E. Shetland basin and Viking graben of the northern North Sea: *J. Geol. Soc. London* **140**, 445–474.

Hamilton, P. J., Fallick, A. E., Macintyre, R. M., and Elliott, S. (1987) Isotopic tracing of the provenance and diagenesis of Lower Brent Group sands, North Sea: in *Petroleum Geology of Northwest Europe,* J. Brooks and K. Glennie, eds., Graham & Trotman Ltd., London, 939–949.

Hancock, N. J. and Taylor, A. M. (1978) Clay mineral diagenesis and oil migration in the Middle Jurassic Brent Sand Formation: *J. Geol. Soc. London* **135**, 69–72.

Haszeldine, R. S., Samson, I. M., and Cornford, C. (1984) Quartz diagenesis and convective fluid movement: Beatrice Oilfield, UK North Sea: *Clay Miner.* **19**, 391–402.

Hoffman, J. and Hower, J. (1979) Clay mineral assemblages as low grade metamorphic geothermometers: Applications to the thrust faulted disturbed belt of Montana, U.S.A.: in *Aspects of Diagenesis,* P. A. Scholle and R. P. Schluger, eds., Soc. Econ. Paleon. Mineral. Spec. Pub. **26**, 55–79.

Hoffman, J., Hower, J., and Aronson, J. L. (1976) Radiometric dating of time of thrusting in the disturbed belt of Montana: *Geology* **4**, 16–20.

Hower, J., Hurley, P. M., Pinson, W. H., and Fairbairn, H. W. (1963) The dependence of K-Ar age on the mineralogy of various particle size ranges in a shale: *Geochim. Cosmochim. Acta* **27**, 405–410.

Hunziker, J. C., Frey, M., Clauer, N., Dallmeyer, R. D., Friedrichsen, H., Flehmig, W., Hochstrasser, K., Roggwiler, H., and Schwander, H. (1986) The evolution of illite to muscovite: Mineralogical and isotopic data from the Glarus Alps, Switzerland: *Contrib. Mineral. Petrol.* **92**, 157–180.

Inoue, A., Kohyama, N., Kitagawa, R., and Watanabe, T. (1987) Chemical and morphological evidence for the conversion of smectite to illite: *Clays & Clay Minerals* **35**, 111–120.

Jennings, S. and Thompson, G. R. (1986) Diagenesis of Plio-Pleistocene sediments of the Colorado River Delta, southern California: *J. Sed. Petrol.* **56**, 89–98.

Jourdan, A., Thomas, M., Brevart, O., Robson, P., Sommer, F., and Sullivan, M. (1987) Diagenesis as the control of the Brent Sandstone reservoir properties in the greater Alwyn area (East Shetland basin): in *Petroleum Geology of Northwest Europe,* J. Brooks and K. Glennie, eds., Graham & Trotman Ltd., London, 951–961.

Lee, M. (1984) Diagenesis of the Permian Rotliegendes Sandstone, North Sea: K/Ar, 180/160, and petrographic evidence: Ph.D. thesis, Case Western Reserve University, Cleveland, Ohio, 346 pp.

Liewig, N., Clauer, N., and Sommer, F. (1987) Rb-Sr and K-Ar dating of clay diagenesis in Jurassic sandstone oil reservoir, North Sea: *Amer. Assoc. Petrol. Geol. Bull.* **71**, 1467–1474.

McHardy, W. J., Wilson, M. J., and Tait, J. M. (1982) Electron microscope and X-ray diffraction studies of filamentous illitic clay from sandstones of the Magnus Field: *Clay Miner.* **17**, 23–39.

McKenzie, D. (1978) Some remarks on the development of sedimentary basins: *Earth Planetary Sci. Letters,* **40**, 25–32.

Middleton, M. F. and Falvey, D. A. (1983) Maturation modeling in Otway Basin, Australia: *Amer. Assoc. Petrol. Geol. Bull.* **67**, 271–279.

Morton, J. P. (1985) Rb-Sr evidence for punctuated illite/smectite diagenesis in the Oligocene Frio Formation, Texas Gulf Coast: *Geol. Soc. Amer. Bull.* **96**, 114–122.

Nadeau, P. H. (1985) The physical dimensions of fundamental clay particles: *Clay Miner.* **20**, 499–514.

Nadeau, P. H. and Bain, D. C. (1986) Composition of some smectites and diagenetic illitic clays and implications for their origin: *Clays & Clay Minerals* **34**, 455–464.

Nadeau, P. H., Wilson, M. J., McHardy, W. J., and Tait, J. M. (1984) Interparticle diffraction: A new concept for interstratified clays: *Clay Miner.* **19**, 757–769.

Pearson, M. J., Watkins, D., and Small, J. S. (1982) Clay diagenesis and organic maturation in northern North Sea sediments: in *Proc. Int. Clay Conf., Oxford, 1978,* M. M. Mortland and V. C. Farmer, eds., Elsevier, Amsterdam, 665–675.

Perry, E. A., Jr. (1974) Diagenesis and the K/Ar dating of shales and clay minerals: *Geol. Soc. Amer. Bull.* **85**, 827–830.

Ramseyer, K. and Boles, J. R. (1986) Mixed-layer illite/smectite minerals in Tertiary sandstones and shales, San Joaquin Basin, California: *Clays & Clay Minerals* **34**, 115–124.

Reynolds, R. C. (1980) Interstratified clay minerals: in *Crystal Structures of Clay Minerals and Their X-ray Identification,* G. W. Brindley and G. Brown, eds., Mineralogical Society, London, 249–304.

Ritter, U. (1985) The influence of time and temperature on vitrinite reflectance: *Organic Geochem.* **6**, 473–480.

Royden, L., Sclater, J. G., and Von Herzen, R. P. (1980) Continental margin subsidence and heat flow: Important parameters in formation of petroleum hydrocarbons: *Amer. Assoc. Petrol. Geol. Bull.* **64**, 173–187.

Sclater, J. G. and Christie, P. A. F. (1980) Continental stretching: An explanation of the post-Mid-Cretaceous subsidence of the Central North Sea basin: *J. Geophys. Research* **85**, 3711–3739.

Środoń, J., Morgan, D. J., Eslinger, E. V., Eberl, D., and Karlinger, M. R. (1986) Chemistry of illite/smectite and end-member illite: *Clays & Clay Minerals* **34**, 369–378.

Steiger, R. H. and Jager, E. (1977) Subcommission on geochronology: Convention on the use of decay constants in geo- and cosmochronology: *Earth Planetary Sci. Letters* **36**, 359–362.

Theisen, A. A. and Harward, M. E. (1962) A paste method for preparation of slides for clay mineral identification by X-ray diffraction: *Soil Sci. Soc. Amer. Proc.* **26**, 90–91.

Thomas, B. M., Moller-Pedersen, P., Whitaker, M. F., and Shaw, N. D. (1985) Organic facies and hydrocarbon distributions in the Norwegian North Sea: in *Petroleum Geochemistry in Exploration of the Norwegian Shelf,* A. G. Dore, S. S. Eggen, P. C. Home, R. Marne, and B. M. Thomas, eds., Norwegian Petroleum Society, Graham & Trotman Ltds., London, 3–26.

Thomas, M. (1986) Diagenetic sequences and K/Ar dating in Jurassic sandstones, central Viking graben: Effects on reservoir properties: *Clay Miner.* **21**, 695–710.

Velde, B., Suzuki, T., and Nicot, E. (1986) Pressure-temperature-composition of illite/smectite mixed-layer minerals: Niger delta mudstones and other examples: *Clays & Clay Minerals* **34**, 435–441.

Waples, D. W. (1980) Time and temperature in petroleum formation: Application of Lopatin's method to petroleum exploration: *Amer. Assoc. Petrol. Geol. Bull.* **64**, 916–926.

Yau, Y. C., Peacor, D. R., and McDowell, S. D. (1987a) Smectite-to-illite reactions in Salton Sea shales: A trans-

mission and analytical electron microscope study: *J. Sed. Petrol.* **57,** 335–342.

Yau, Y. C., Peacor, D. R., Essene, E. J., Lee, J. H., Kuo, L. C., and Cosca, M. A. (1987b) Hydrothermal treatment of smectite, illite, and basalt to 460°C: Comparison of natural with hydrothermally formed clay minerals: *Clays & Clay Minerals* **35,** 241–250.